

## Simple PV battery charger without MPPT based on SEPIC converter

Hristo Antchev, Anton Andonov

*This article describes a specific implementation of a SEPIC converter for charging an accumulator battery from a photovoltaic panel and which is characterized by simple control without MPPT. Here are presented some basic mathematical dependencies on the transmission functions that can be used in the implementation of the control and regulation systems of other DC-to-DC converters without galvanic isolation. The article shows a schematic diagram and the way it work. Here are presented experimental research results as well as conclusions on the feasibility of the presented scheme and the dependencies.*

**Keywords** – battery, charger, control, converter, photovoltaic.

*Зарядно устройство за акумулаторна батерия от фотоволтаичен панел на основата на SEPIC преобразувател (Христо Анчев, Антон Андонов). В статията се разглежда зарядно устройство за акумулаторна батерия на базата на SEPIC преобразувател (Single Ended Primary Inductance Converter). Устройството се характеризира с опростена и надеждна структура без следене на точката на максимална мощност MPPT (Maximum Power Point Tracking). Изведени са основните предавателни функции за входната мощност от фотоволтаичния панел по отношение на изходното съпротивление на преобразувателя, неговото входно напрежение и коефициента на запълване на управляващите импулси за транзистора. Представена е пълната принципна схема на зарядното устройство и е пояснена работата ѝ. Зарядното устройство реализира алгоритъм на зареждане с константен ток и ограничение по напрежение за акумулаторната батерия. Представени са осцилограми от експериментални изследвания при начално зареждане, напълно заредена батерия, както и при сработване на защитата по ток при различни напрежения на фотоволтаичния панел.*

### Introduction

With the widespread use of renewable energy sources, various applications of energy storage elements have been developed - supercapacitor and mainly accumulator batteries [1], [2]. DC-to-DC converters with or without galvanic isolation are used for their charging. For those without galvanic isolation, the basic application is for the SEPIC Converter and more rarely Zeta converter [3], [4], [5]. A research on a system of parallel co-working converters is done in [6]. The volt-ampere characteristic of photovoltaic panels, changing under temperature and solar radiation, generally requires Maximum Power Point Tracking (MPPT) for optimal power utilization. For this purpose, there are different methods described, for example, in [7], [8], with application example for SEPIC converter [9]. Significantly more limited are the descriptions of MPPT-free variants, popularly called Pulse Width

Modulation (PWM) variants. They are characterized by a simple solution and lower price. At the same time, there are researches showing that, for example, in the temperature range of the panel and for lower power, the option without MPPT is more inexpensive and is almost as efficient as the one with MPPT [10].

This study presents a research of a SEPIC converter for charging an accumulator battery from a photovoltaic panel without MPPT. For creating the circuit diagram are used some of the ideas presented in [11], [12]. Part II presents the mathematical link between the major values. A description of the circuit diagram is made in Part III. The experimental results are shown in Part IV.

### Mathematical description

Assuming that the energy efficiency of the converter is equal to 1, then:

$$(1) \quad P_O = P_I,$$

$$(2) \quad U_O \cdot I_O = U_I \cdot I_I$$

where  $P_O$  – output power,  $P_I$  - input power,  $U_O$  - output voltage,  $I_O$  - output current,  $U_I$  - input voltage,  $I_I$  - input current.

$$(3) \quad \frac{U_O}{U_I} = K = \frac{\delta}{1-\delta}; \quad \delta = \frac{t_{ON}}{T},$$

where  $\delta$  is the duty cycle,  $t_{ON}$  - the time the transistor is switched on,  $T$  - the period of operation.

From (2) and (3) follows

$$(4) \quad \frac{I_O}{I_I} = \frac{1}{K} = \frac{1-\delta}{\delta}$$

and from (3) and (4)

$$(5) \quad \frac{R_I}{R_O} = \left(\frac{1}{K}\right)^2 = \left(\frac{1-\delta}{\delta}\right)^2$$

Therefore, for the input power can be recorded:

$$(6) \quad P_I = \frac{U_I^2}{R_I} = U_I^2 \cdot \left(\frac{\delta}{1-\delta}\right)^2 \cdot \frac{1}{R_O}$$

The full input power  $P_I$  differential is:

$$(7) \quad dP_I = 2 \cdot U_I \cdot \left(\frac{\delta}{1-\delta}\right)^2 \cdot \frac{1}{R_O} \cdot dU_I + 2 \cdot \frac{\delta}{(1-\delta)^3} \cdot U_I^2 \cdot \frac{1}{R_O} \cdot d\delta - \frac{1}{R_O^2} \cdot U_I^2 \cdot \left(\frac{\delta}{1-\delta}\right)^2 \cdot dR_O$$

Here can be figured the change of input power  $P_I$  at the changing of one of the values  $U_I$ ,  $\delta$ ,  $R_O$  and the invariable value of the other two.

For example, in relation to the variation of the output resistance:

$$(8) \quad dP_I = - \left[ \frac{U_I}{R_O} \cdot \left(\frac{\delta}{1-\delta}\right)^2 \right] \cdot dR_O = - \left[ \frac{U_O}{R_O} \cdot \left(\frac{1-\delta}{\delta}\right) \cdot \left(\frac{\delta}{1-\delta}\right) \right]^2 \cdot dR_O = -I_O^2 \cdot dR_O$$

Finally:

$$(9) \quad dP_I = -I_O^2 \cdot dR_O$$

In relation to input voltage changes:

$$(10) \quad dP_I = 2 \cdot U_I \cdot \left(\frac{\delta}{1-\delta}\right)^2 \cdot \frac{1}{R_O} \cdot dU_I = 2 \cdot \frac{U_O}{R_O} \cdot \frac{\delta}{1-\delta} \cdot dU_I = 2 \cdot I_O \cdot \frac{\delta}{1-\delta} \cdot dU_I = 2 \cdot I_I \cdot dU_I$$

or:

$$(11) \quad dP_I = 2 \cdot I_O \cdot \frac{\delta}{1-\delta} \cdot dU_I = 2 \cdot I_I \cdot dU_I$$

Regarding the changes in the duty cycle:

$$(12) \quad dP_I = 2 \cdot \frac{\delta}{(1-\delta)^3} \cdot U_I^2 \cdot \frac{1}{R_O} \cdot d\delta = 2 \cdot \frac{U_O^2}{\delta \cdot (1-\delta)} \cdot \frac{1}{R_O} \cdot d\delta = 2 \cdot \frac{I_O \cdot U_O}{\delta \cdot (1-\delta)} \cdot d\delta = 2 \cdot \frac{P_O}{\delta \cdot (1-\delta)} \cdot d\delta$$

Finally:

$$(13) \quad dP_I = 2 \cdot \frac{P_O}{\delta \cdot (1-\delta)} \cdot d\delta$$

Fig. 1 shows the approximate change of the output current and the output voltage at charging algorithm with constant current and voltage limits.

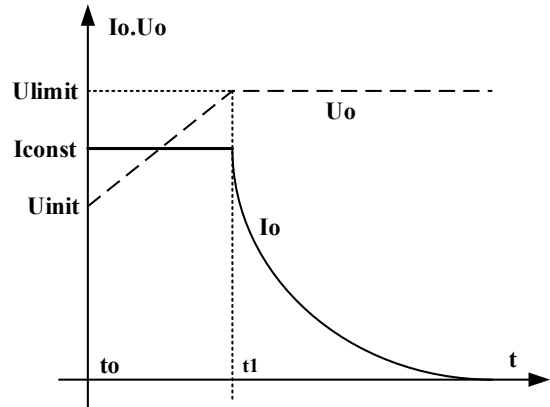


Fig.1. Change of output current and output voltage.

The initial power corresponds to the moment  $t_0$ :

$$(14) \quad P_{init} = U_{init} \cdot I_{const}$$

The biggest output power value will be at the moment  $t_1$ :

$$(15) \quad P_{limit} = U_{limit} \cdot I_{const}$$

For example, for a 12V nominal voltage accumulator and 50Ah capacity, the typical values are:

$$U_{init} = 10V, U_{limit} = 13.8V, I_{const} = 5A$$

For the interval  $t_0 \div t_1$  the change of the output resistance is

$$dR_O \approx \Delta R_O = \frac{U_{init} - U_{limit}}{I_{const}} = \frac{10 - 13.8}{5} = -0.76\Omega.$$

For the change of the input power assuming that the energy efficiency is equal to 1, the formula (9) leads to  $dP_I \approx \Delta P_I = -5^2 \cdot (-0.76) = 19W$ .

A similar result is achieved in the following way

$$\Delta P_I = P_{t_1} - P_{t_0} = U_{limit} \cdot I_{const} - U_{init} \cdot I_{const} = 13.85 - 10.5 = 19W$$

The presented dependencies can also be used in other non-galvanic isolation converters, in which the input and output voltages are connected with (3) - buck/boost, Cuk converter, Zeta converter.

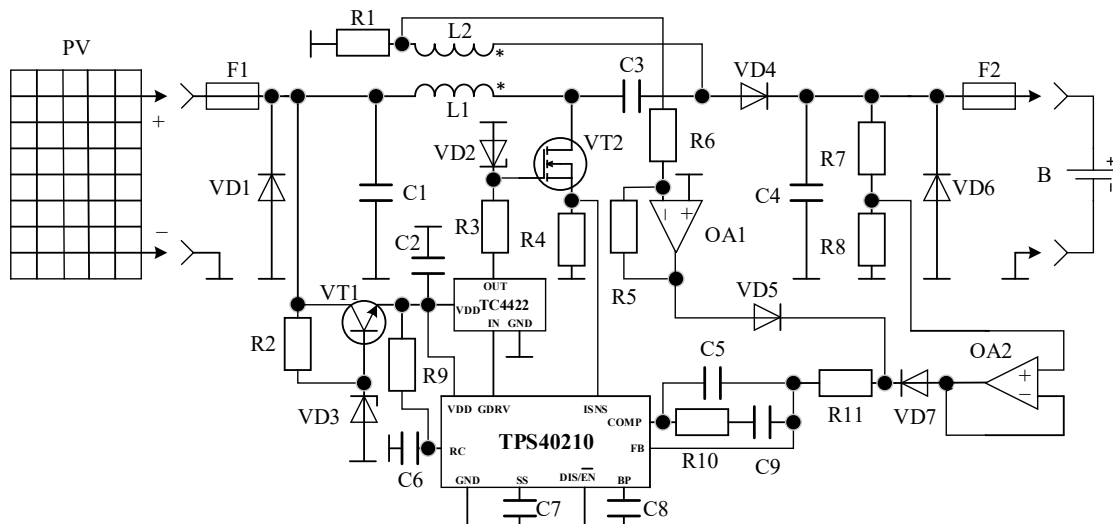


Fig.2. Schematic diagram of the converter.

### Scheme and description of the operation

The schematic diagram is shown in Fig. 2. The main elements of the power scheme of the SEPIC converter are:  $C1$ ,  $L1$ ,  $L2$ ,  $VT2$ ,  $C3$ ,  $VD4$ ,  $C4$ .

The operation control is done through the integrated circuit TPS40210 [13]. To its output at the GDRV transistor is connected TC4422 driver [14]. The supply voltages VDD for the two integrated circuits are obtained by the stabilizer with the elements  $VT1$ ,  $R2$ ,  $VD3$ , and  $C2$ . The frequency of operation of the converter is set with the elements  $R9, C6$  [13] and in this case, it is selected equal to 100 kHz. A battery-charging mode with constant current and voltage limitation is implemented. The elements of the voltage feedback circuit are  $R7$ ,  $R8$ ,  $OA2$ ,  $VD7$ , with the output

voltage value set to 3.8V. The value of the output charging current is monitored indirectly via  $R1$ , and the current feedback circuit also includes  $OA1$ ,  $R6$ ,  $R5$ ,  $VD5$ . The indicators of the closed loop system (accuracy, sustainability, transition process parameters, etc.) are established by the elements connected between the COMP and FB terminals:  $R11$ ,  $R10$ ,  $C5$ , and  $C9$ . The connected capacitor  $C7$  to SS terminal determines the soft start time of the converter [13]. Additionally, the following protections are implemented: current overload and short-circuit at the output protections (via the resistor  $R4$  connected to ISNS terminal); change of polarity of the photovoltaic panel or the battery protections (respectively with  $F1$ ,  $VD1$  and  $F2$ ,  $VD6$ ). For the design of the elements of the power circuit diagram can be used [15] for example.

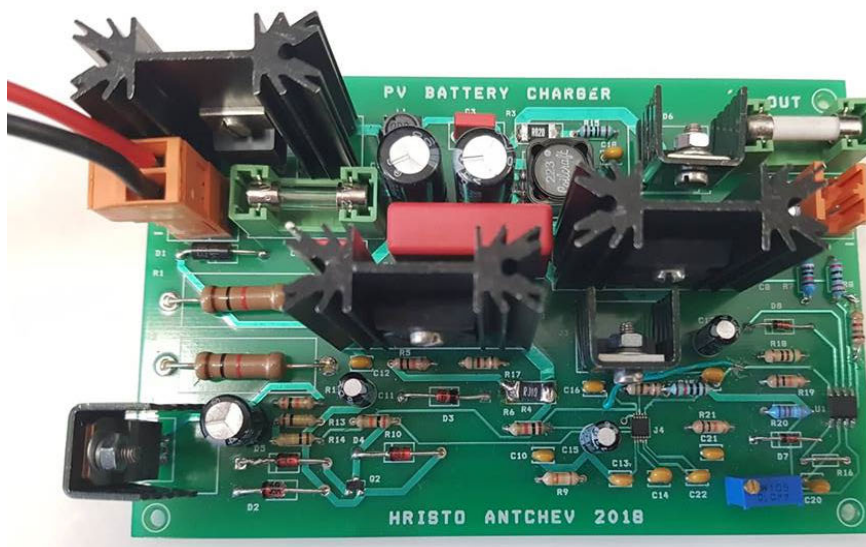


Fig.3. Appearance of the converter.

## Experimental results

Fig.3 shows the appearance of the converter. The operating range of the input voltage is  $9V - 36V$ , as the low limit is determined by the minimal supply voltage of TPS40210.

The experiment is done with a  $12V/50Ah$  accumulator powered by a PV-PV120-1-18 photovoltaic panel with the following values: maximum power -  $P_{MAX} = 120W$ , open circuit voltage -  $V_{OC} = 22V$ , short circuit current -  $I_{SC} = 7.34A$ , and voltage at maximum power point -  $V_{MPP} = 17.6V$ , and current at maximum power point -  $I_{MPP} = 6.8A$ .

Fig. 4, Fig. 5 and Fig. 6 show some oscillograms of the experiments.

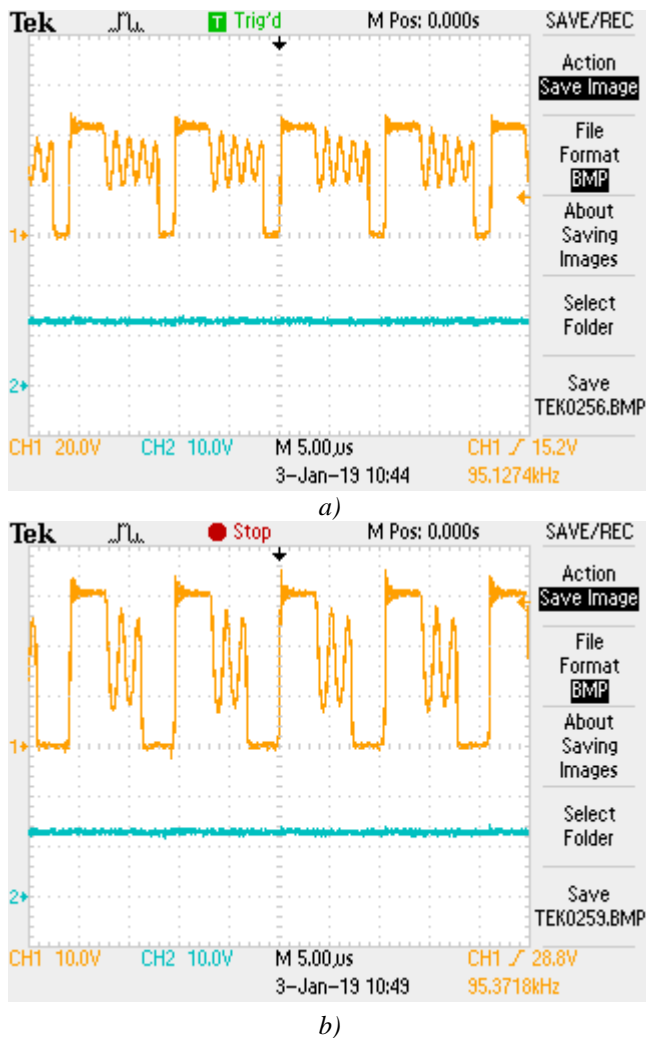


Fig.4. CH1 – drain-source voltage of VT2, CH2 – accumulator battery voltage, a) input voltage 22V, b) input voltage 17V.

The experiments are made at input voltages around the maximum power point. CH2 on Fig. 4 shows that

the battery voltage has reached the limit of  $\approx 13.8V$  and the charging current has dropped to  $0.35A$  (measured value).

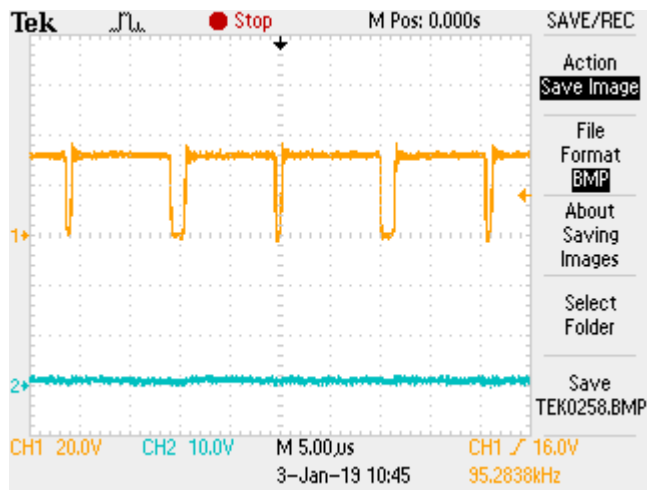
CH2 on Fig. 5 shows that the battery voltage is at the beginning of the charge  $\approx 10V$  and the charging current is constant  $5A$  (measured value).



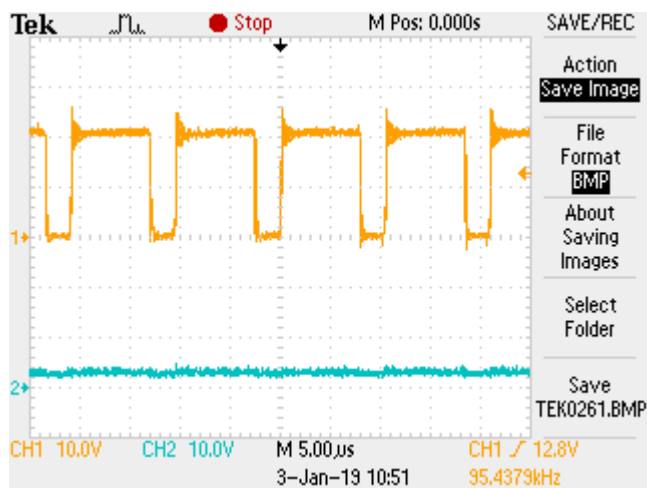
Fig.5. CH1 - drain-source voltage of VT2, CH2 - accumulator battery voltage, a) input voltage 20V, b) input voltage 13V

Fig. 6 shows the oscillograms at short circuit at the output, i.e. the short-circuit protection. The current value at which the protection starts working is  $\approx 5.5A$ . Fig. 6a shows that the duty cycle of the control impulses for the transistor has been reduced to a minimum value (at the time of switching on the transistor), resulting in a decrease of the output voltage approximately to 0. Therefore, the short-circuit current is measured about  $6A$  (measured value). Fig. 6b shows that the duty cycle of the controlling impulses of the

transistor has not yet dropped to minimum value (at the time of switching on the transistor), resulting in a decrease in the output voltage but not yet equal to 0. At this, the current is measured around 5.8A.



a)



b)

Fig.6. CH1 - drain-source voltage of VT2, CH2 – accumulator battery voltage  
a) input voltage 13V, b) input voltage 11V

### Conclusion

For the analyzed in the present study SEPIC converter are obtained the transmission functions of the input power to the output resistance (9), the input voltage (11) and the duty cycle of the control impulses (13) that can be used in various methods and circuits. Here is described a concrete implementation of an accumulator battery charge converter of a photovoltaic panel without MPPT and a schematic diagram and experimental results are presented.

### REFERENCES

- [1] D. Ganesh, S. Moorthi, H. Sudheer, A Voltage Controller in Phot-Voltaic System with Battery Storage for Stand-Allone Applications, International Journal of Power Electronics and Drive Systems, Vol.2, No.1, 2012, pp.9-18.
- [2] N. Sujitha, S. Krithiga, RES based EV battery charging systems: A review, Renewable and Sustainable Energy Reviews, 75(2017), pp.978-988.
- [3] Microchip Technology, High-Power CC/CV Battery Charger Using an Inverse SEPIC(Zeta) Topology, AN1467, 2012.
- [4] Texas Instruments, Jeff Falin, Designing DC/DC Converters based on SEPIC Topology, Analog Applications Journal, 4Q, 2008, derived from www.ti.com/aaj.
- [5] S.J.Chiang, H.J.Shieh, M.C.Chen, Modeling and Control of PV Charger System With SEPIC Converter, IEEE Transactions on Industrial Electronics, Vol.56, Issue 11, 2009, pp.4344-4353, DOI:10.1109/TIE.2008.2005144.
- [6] Antchev H., Investigation of systems of power electronic converters with common output DC voltage, PhD thesis, S., 2012, (in Bulgarian).
- [7] B. Bendib, H. Belmili, F. Krim, A survey of the most used MPPT methods: Conventional and advanced algorithms applied for photovoltaic systems, Renewable and Sustainable Energy Reviews, Vol.45, May 2015, pp.637-648.
- [8] S.E. Babaa, M. Armstrong, V. Pickert, Overview on Maximum Power Point Tracking Control Methods for PV Systems, Journal of Power and Energy Engineering, 2014,2 pp.59-72.
- [9] T. Ramalu, M.A.M. Radzi, M.A.A.M. Zainuri, N.I.A. Wahab, R.Z.A. Rahman, A Photovoltaic-Based SEPIC Converter with Dual Fuzzy Maximum Power Point Tracking for Optimal Buck and Boost Operations, Energies, 9(8), 2016, DOI:10.3390/en9080604.
- [10] Victron Energy B.V., Which Charge Controller: PWM or MPPT?, 24 June, 2014, The Netherlands, derived from www.victronenergy.com.
- [11] Texas Instruments, Fast Capacitor Charger with SEPIC Topology (42V to 52Vin, 160V/180Vout@900 mA) Reference Design, derived from www.ti.com/tool/PMP30162.
- [12] Texas Instruments, 20W SEPIC Low-Cost Lead Acid Battery Charger reference Design, derived from www.ti.com/tool/PMP10081.
- [13] Texas Instruments, TPS4021x 4.5V to 52V Input Current Mode Boost Controller, SLUS772F, March 2008-Revised March 2015.
- [14] Microchip Technology, TC4421/TC4422, 9A High-Speed MOSFET Drivers, DS20001420F, 2002-2013.
- [15] Texas Instruments, Designing a SEPIC Converter, Application Report, SNVA168E-May 2006-Revised April 2013.

---

**Dr. H. Antchev** awarded Bachelor and Master degrees at Technical University – Sofia, Bulgaria, in specialization “Power Electronics. He is a senior assistant at the University of Chemical Technology and Metallurgy in Sofia. He works in the field of design of power electronic converters and control systems.

*e-mail: hristo.antchev@gmail.com.*

**Assoc. Prof. Dr. A. Andonov** is Head of the Department of Electrical Engineering and Electronics at the University of Chemical Technology and Metallurgy in Sofia. He graduated from the Technical University of Sofia, specialty electrical power supply and electrical equipment.

*e-mail: andonov@uctm.edu*

**Received on: 11.02.2019**

---

## **THE FEDERATION OF THE SCIENTIFIC-ENGINEERING UNIONS IN BULGARIA /FNTS/**

is a professional, scientific - educational, nongovernmental, nonpolitical, nonprofit association of legal entities - professional organizations registered under the Law on non-profit legal entities, and their members are engineers, economists and other specialists in the fields of science, technology, economy and agriculture.

FNTS has bilateral cooperation treaties with similar organizations in multiple countries.

FNTS brings together 19 national associations – Scientific and Technical Unions (STU), 34 territorial associations, which have more than 15 000 professionals across the country.

FNTS is a co-founder and member of the World Federation of Engineering Organizations (WFEO).

FNTS is a member of the European Federation of National Engineering Associations (FEANI), and a member of the Standing Conference of engineering organizations from Southeast Europe (COPISEE), UN Global Compact, European Young Engineers (EYE). The Federation has the exclusive right to give nominations for the European Engineer (EUR ING) title.

**Contacts:** 108 Rakovsky St., Sofia 1000, Bulgaria

**WEB:** <http://www.fnts.bg>

**E-mail:** [info@fnts.bg](mailto:info@fnts.bg)